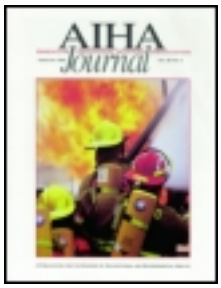

AIHA Journal
Publication details, including instructions for authors and subscription information:
http://www.tandfonline.com/loi/uaih20

Applying Open-Path FTIR with a Bi-Beam Strategy to Evaluate Personal Exposure in Indoor Environments: Experimental Results of a Validation Study

Chang-Fu Wu [a], Michael G. Yost [a], Janice Varr [a] & Ram A. Hashmonay [b]
[a] Department of Environmental Health, University of Washington, Seattle, WA 98195
[b] ARCADIS Geraghty & Miller, Research Triangle Park, NC 27709

Available online: 04 Jun 2010

To cite this article: Chang-Fu Wu, Michael G. Yost, Janice Varr & Ram A. Hashmonay (2003): Applying Open-Path FTIR with a Bi-Beam Strategy to Evaluate Personal Exposure in Indoor Environments: Experimental Results of a Validation Study, AIHA Journal, 64:2, 181-188

To link to this article: http://dx.doi.org/10.1080/15428110308984807

AIHA Journal 64:181–188 (2003) Ms. #278

Applying Open-Path FTIR with a Bi-Beam Strategy to Evaluate Personal Exposure in Indoor Environments: Experimental Results of a Validation Study

AUTHORS
Chang-Fu Wu[a]
Michael G. Yost[a]
Janice Varr[a]
Ram A. Hashmonay[b]

[a]Department of Environmental Health, University of Washington, Seattle, WA 98195
[b]ARCADIS Geraghty & Miller, Research Triangle Park, NC 27709

This study evaluated the performance and feasibility of using open-path Fourier transform infrared (OP-FTIR) with a bi-beam strategy to assess personal exposures in workplaces. The bi-beam strategy combines a long beam and a short beam measurement to calculate the average concentration level of the segmented region. A series of experiments was conducted with six human subjects at two workstations inside a chamber. A bi-beam geometry was set up for each workstation. Each subject repeatedly performed two tasks (9 min/task), which were designed to simulate a painting and an assembly task. For each task a tracer gas (N_2O) was released from a point source near the subject. During each task, while the OP-FTIR collected the N_2O spectrum, bag samples were collected simultaneously at nose and lapel height. Statistical data analysis applied a general linear model with the bag samples as the dependent variable. Results show that the locations, tasks, and subjects are not significant factors when using OP-FTIR measurements with the bi-beam strategy to estimate personal exposure at the nose height. The model used in this study fits the data reasonably well ($R^2=0.87$), and when it is compared with a second set of experimental data, the bias is 0.7 ppm (3%) and the precision is 5.5 ppm. This study demonstrates that the bi-beam sampling strategy may offer a new approach for applying OP-FTIR to industrial hygiene monitoring.

Keywords: beam geometry, gamma model, open-path FTIR, personal exposure

This research was partially supported by the National Institute for Occupational and Safety Health (NIOSH) grant RO1OH02660 and by the Consortium for Risk Evaluation with Stakeholder Participation (CRESP) through Department of Energy Cooperative Agreement #DE-FC01–95EW55084. This does not constitute an endorsement by NIOSH or DOE of the views expressed in this article.

Open-path Fourier transform infrared (OP-FTIR) is an optical remote sensing technique that can be used to identify and quantify vapors and gases for air sampling purposes.[1] Most of the early studies have focused on applications in ambient environments. One example is the remote optical sensing of emissions system developed by the U.S. Environmental Protection Agency.[2]

For workplace applications, OP-FTIR offers some features that industrial hygienists may find useful.[3,4] The infrared spectra produced by the OP-FTIR system can provide real-time information for mixtures of compounds in the air and also can be used to identify unexpected compounds. Typically, a few seconds of spectral scans are sufficient for quantification of known compounds with low detection limits. This real-time information is especially useful when the contaminants have acute effects, and the OP-FTIR then can be set up as a warning system. In addition, because all the information is contained in the spectra that are stored digitally, one can reevaluate the data later if more advanced analysis methods are developed.

However, there also are some disadvantages that limit the application of this technique. First, it is not always easy to collect a clean background spectrum, which serves as a reference that can compensate for instrument factors and some environmental factors.[4] Sometimes, it may be impractical or impossible to obtain a clean air

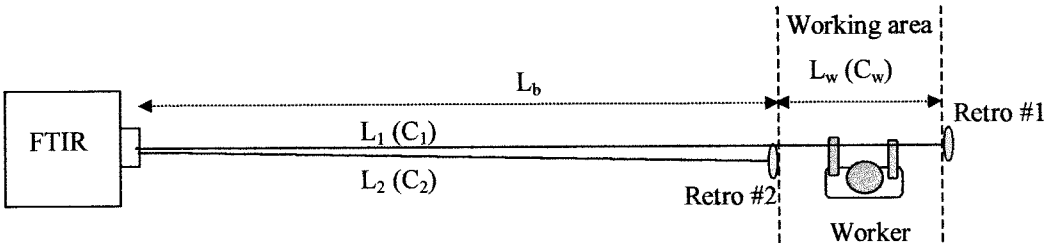

FIGURE 1. Concepts of the bi-beam geometry. L_1 represents the sampling beam, and L_2 represents the reference beam. L_w is the region of interest for assessing personal exposures.

spectrum during or between working shifts. Second, an OP-FTIR system can provide only path-integrated data.[4,5] Dividing the path-integrated data by the path length gives path-averaged concentrations along the measured beam path, but does not tell how the contaminants are distributed. For industrial hygiene purposes, it would be better to have spatially resolved data over the sampled path to further investigate exposures in the workplace.

In the past two decades, several research groups have applied computed tomography (CT) techniques to mathematically calculate and obtain spatially resolved measurements with the OP-FTIR beam data.[4,6–14] These studies have theoretically and experimentally validated the agreement between the measurements from area sampling and the OP-FTIR with CT. However, few studies have provided data on the correlations between the OP-FTIR and personal sampling.[15,16] Traditional personal sampling devices require workers to wear pumps that store the samples in bags or charcoal tubes, and the sampling inlet is located in the breathing zone. The results usually are time-integrated data. Although some real-time monitoring devices can provide personal data with good temporal resolution, most of these devices are useful for only one or two specific compounds. These limitations lead us to investigate the application of using OP-FTIR to assess personal exposure because of the advantages (e.g., real-time information, identifying mixtures) mentioned previously. Furthermore, workers are not required to wear bulky sampling devices because of the remote sensing ability of the OP-FTIR.

This study developed and applied a "bi-beam strategy" with an OP-FTIR system to evaluate personal exposures and compared the results to bag samples. The bi-beam strategy uses the spectra collected from a long beam path and a short beam path to calculate the average concentration level of the segmented region. The development of this sampling strategy is presented in the following section. A series of experiments was conducted with six human subjects in a ventilation chamber to validate this approach. The bi-beam strategy does not require obtaining clean background spectra and also can provide segmenting information along the measured beam path.

METHODOLOGY

A Bi-Beam Sampling Strategy

The concept of the bi-beam strategy is illustrated in Figure 1. Retroreflectors are placed at the two ends of a working area, and the average concentration (C_w in Figure 1) in the working area (L_w in Figure 1) between the two retroreflectors is found. The longer beam path, L_1, serves as a sampling beam, and the shorter beam path, L_2, serves as a reference beam. The OP-FTIR scans the two beam paths alternately and rapidly, thus measuring path integrated concentrations C_1 and C_2 over paths lengths L_1 and L_2, respectively. Because the measurements over paths L_1 and L_2 are very close to each other in space and time, it can be assumed that the L_2 represents the beam segment L_b of beam L_1. The directional shift required to scan from one retroreflector to another could introduce some errors, especially when the concentration gradients are significant. To minimize the errors, Retroreflector 2 should be placed as close to Retroreflector 1 as possible on the same line without blocking the beampath to the Retroreflector 1. Alternatively, directional errors could be completely avoided by moving Retroreflector 2 in and out of a single stationary beam path to create the reference beam.

The Beer-Lambert law[1] was applied to write the concentration readings in terms of absorbance along the beam paths, obtaining:

$$A_1 = -\log\left(\frac{I_1}{I_0}\right) = \alpha(L_w C_w + L_2 C_2) \quad \text{for the path to retro 1} \qquad (1)$$

$$A_2 = -\log\left(\frac{I_2}{I_0}\right) = \alpha L_2 C_2 \quad \text{for the path to retro 2} \qquad (2)$$

where α is the absorption coefficient of the contaminants, I_0 represents the usual uncontaminated background transmission spectrum, and I_1, I_2 correspond to the sample spectra measured for the beam segments. Writing the absorbance for the worker's breathing zone A_W shows:

$$A_w = \alpha L_w C_w = A_1 - \alpha L_2 C_2 = A_1 - A_2 = -\log\left(\frac{I_1}{I_2}\right) \qquad (3)$$

Thus, the absorbance spectrum (and hence the average concentration of contaminants for the worker's breathing zone segment) is found from the ratio of the two sampled spectra along each beampath. Also notice from Equation 3 that the background spectrum I_0 is no longer needed.

EXPERIMENTAL METHODS

Wind Tunnel

The experiments were conducted in a chamber, 11.1 m long, 5.4 m wide, and 2.4 m high, as described in Wu et al.[13] The chamber is equipped with an inlet fan and an outlet fan that can provide controlled ventilation in a plug-flow arrangement. Two worktables (0.9 m wide by 0.7 m long by 0.8 m high) were placed about 0.4 m apart across the width of the tunnel (Figure 2).

Subjects and Simulation Tasks

Six subjects (four men and two women) participated in the experiments. Participation of human volunteers was monitored and

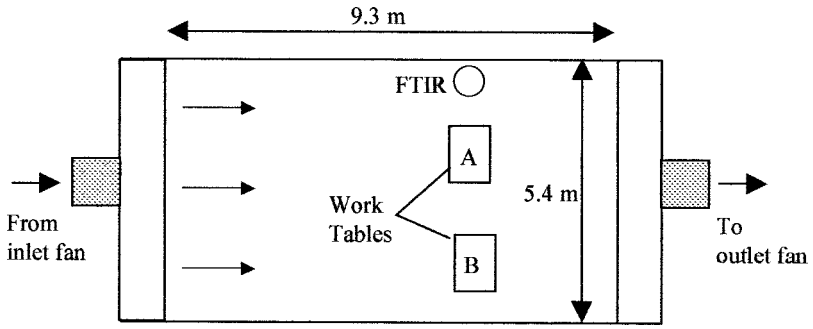

FIGURE 2. Top view of the experimental setup

approved by the University of Washington Human Subjects Committee. All trials were completed without a violation of protocol or loss of data. The subjects repeatedly performed two tasks during the experiments. The tasks were designed to simulate a painting and an assembly task, which could be found in industry. For each task a spherical diffuser released pure nitrous oxide (N_2O) (Praxair, Seattle, Wash.) as the tracer gas. The flow rate of gas was regulated with a mass flow controller (Sierra Instruments, Monterey, Calif.).

For the painting task the subject was asked to simulate the painting of a 20.3 cm × 24.1 cm × 10.2 cm cardboard box (no paint was actually used). The gas diffuser was fixed in place inside this box, which was punched with 0.3 cm diameter holes on all six sides to allow the gas to escape. A 2.5-cm paintbrush was provided as well as a 15.2-cm diameter "paint" can. The subject was instructed to paint the box at a speed of approximately 1–2 brushstrokes per sec, dipping the paintbrush into the can as appropriate. Subjects were instructed to hold the box at belt height as a means of preventing overexposure to N_2O gas. In this task the subject was holding and interacting with the N_2O source.

For the assembly task a 21.0 cm × 15.9 cm × 11.4 cm high cardboard box containing LEGO® building bricks was situated next to a 10.8 cm high, 7.6 cm diameter can containing the spherical N_2O gas diffuser. Subjects were instructed to build any structure they wished, but to draw the LEGO building bricks from the box every 10–15 sec. For this task the N_2O source was not handled, but rather remained fixed near the subject's workspace on the tabletop.

OP-FTIR and Bi-Beam Geometry Description

The OP-FTIR instrument was custom-built by ETG (Environmental Technologies Group, Norcross, Ga.) based on a modified Nicolet (Nicolet Instrument Corp., Madison, Wis.) ST-1 optical bench. This instrument is described in detail in Wu et al.[13] It had a liquid nitrogen cooled mercury-cadmium-telluride detector and a unistatic design with the IR source, interferometer, and detector housed in one box. A remote retroreflector was needed to return the external beam back over the same path to the spectrometer. The OP-FTIR instrument was mounted on a scanner that could direct the IR beam over 360° rotation and ±30° elevation controlled by a Unidex stepper-motor computer controller (Aerotech, Inc., Pittsburgh, Pa.). The OP-FTIR system was operated through an MS-DOS® PC with a Pentium® 133 MHz processor.

The OP-FTIR was placed near the tunnel wall, approximately 0.9 m away from the nearest worktable. Three retroreflectors were situated around each worktable as shown in Figure 3. One retroreflector was attached to a metal post fixed to the edge of each tabletop closest to the FTIR (retro 1 or 4). The beampath from the FTIR to this retro served as the reference beam at that worktable. Two other retroreflectors were fixed one above the other

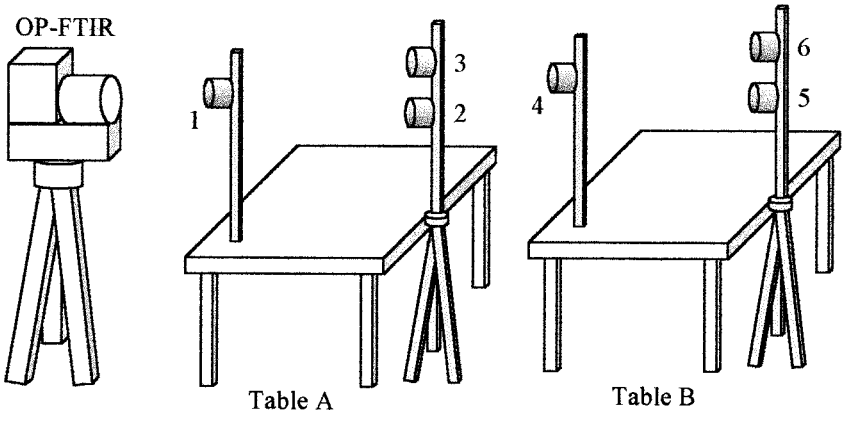

FIGURE 3. Side view of the experimental setup. The beampath from the FTIR to retroreflectors 1 and 4 served as the reference beams. The beampath from the FTIR to retroreflectors 2 and 5 represented the personal exposures at lapel height. The beampath from the FTIR to retroreflectors 3 and 6 represented personal exposures at nose height.

on tripods located at the opposite end of each worktable. The lower retroreflector (retro 2 or 5) was positioned to create a beampath across the subject's lapel area (''low beam'') whereas the higher retroreflector (retro 3 or 6) created a beampath crossing in front of the subject at nose height (''high beam'').

Personal Exposure with Bag Samples

Two sampling trains were set up to collect air samples from areas near the subject's right lapel and nose. Each train consisted of a Spectrex PAS-3000 personal air sampling pump (Redwood City, Calif.) located outside the tunnel at a monitoring station, rigged to approximately 15 m of 3/16-inch (interior diameter) Tygon® tubing. One tube end was taped to the right lapel area of each subject, on the upper chest approximately 3 inches from the top of the right shoulder. The second tube was attached to safety glasses worn by the subject and adjusted so the tube end rested on the right side of the subject's nose. The sampling pumps operated at a flow rate of approximately 240 mL/min. All pumps were calibrated with a Gilian Gilibrator (Gilian Instruments, Caldwell, N.J.).

Air samples were collected into 12-L Tedlar® bags (SKC, Eighty Four, Pa.), which were later analyzed for N_2O using a calibrated B&K IR photoacoustic detector (Brüel and Kjær, model 1302). The collection efficiency of each sampling train was tested by drawing a N_2O/air mixture of known concentration through the entire sampling train into an evacuated sampling bag and then analyzing this bag for N_2O using the B&K detector. The collection efficiency for both sampling trains exceeded 95%.

Calibration Experiment

To make sure the measurements from the OP-FTIR and the bag samples were comparable with each other, calibration experiments were conducted before the major exposure experiments. A homogeneous concentration of N_2O was created in the chamber by releasing the N_2O gas into the inlet duct of the wind tunnel just upstream of the inlet fan. The emission rate was set at approximately 3.5 L/min. Lapel and nose sampling trains were hooked up to a 158-cm tall department store-type female mannequin. While the OP-FTIR scanned with the bi-beam geometry mentioned above, both the lapel and nose height sampling bags were collected. The data collection procedure was the same as the procedure in the main exposure experiments described below. Four trials of calibration experiments were conducted.

Main Exposure Experiment

All experiments were conducted with the wind speed set approximately at 13.5 m/min. A gas flow rate, regulated by a Sierra Sidetrak III mass flow controller and a Series 900 Flo-Box™ (Sierra Instruments, Carmel Valley, Calif.), was set individually for each subject between 75 and 108 mL/min based on his or her height. The flow rate was chosen to ensure that the subject's average exposure did not exceed the threshold limit value of 50 ppm.

Each experimental session lasted approximately 1.75 hours and consisted of eight rounds. During each round the subject performed one task at a given worktable for approximately 9 min. A starting task/worktable location combination was randomly assigned to each subject. During each round, lapel and nose height bag samples were collected while the OP-FTIR repeatedly scanned the three retroreflectors situated at that worktable. At the end of the first round a 1-min time interval followed in which the subject moved to the opposite task/worktable and stood in place, allowing the wind to stabilize around the subject and worktable. This period also provided time for lingering gas at the previous worktable to be carried off by the wind stream. No sampling was conducted during this 1-min interval. Round 2 then began, and the subject performed the new task at the second worktable for approximately another 9 min while two new bag samples were collected and OP-FTIR sampling resumed. At the end of round 2 the subject returned to the initial task/worktable, a 1-min wait ensued, and the process was repeated for rounds 3 and 4. At the conclusion of round 4 the subject was allowed to rest and/or leave the wind tunnel for 5 or 10 min, during which time the tasks were switched to the opposite worktable. Rounds 5 through 8 proceeded similarly to rounds 1 through 4. After eight rounds were completed, two repeated sets of measurement data were obtained for the four possible task/worktable combinations (assembly/table A, painting/table A, assembly/table B, and painting/table B). The subject returned on another day and repeated the same process, beginning with the same initial task/worktable combination as before.

During any one round a 9-min bag sample was simultaneously collected by both the lapel and nose sampling trains. This process was repeated for each round, so that at the end of eight rounds, 16 sample bags were collected, half each from the lapel and nose area sampling trains.

OP-FTIR scanning for any one round was done sequentially, beginning with the high retroreflector, proceeding to the reference retroreflector, and ending with the low retroreflector. This sequencing ensured that the reference beam was collected equally close in time to each sample beam. This scanning cycle was repeated 10 times, resulting in the collection of 10 spectra per retroreflector during any one round. Each retroreflector was scanned for approximately 14 sec, and a 4-sec interval was allowed for the FTIR to aim at the next target retroreflector.

Data Processing

Each OP-FTIR spectrum was collected at 2 cm^{-1} spectral resolution and quantified by Nicolet PC/IR™ software with the classic least squares method.[17] A double-beam spectrum was obtained by using the reference single beam spectrum as the background spectrum and using either the nose-height or the lapel-height single beam spectrum as the single beam sample spectrum. The quantification method was the same as was used in Wu et al.[13] The spectral range used for N_2O quantification was 2120–2270 cm^{-1}. The reference spectra for quantification (2 cm^{-1} resolution) were obtained from the EXAMS library (Expert Air Monitoring System, Automotive Safety and Health Research, General Motors Corp.). The quantification method used two reference spectra at 100 ppm-m and 336 ppm-m for N_2O.

Statistical Analysis

General linear modeling (GLM) was applied for the data statistical analysis. Two empirical models were considered here:

$$\text{Model 1:}\quad \log(C_{BAG}) = \text{intercept} + \beta_1 \log(C_w) + \beta_2 \text{LOC} + \beta_3 \text{TASK} + \beta_{4i} \text{SUBJ}_i \qquad (4)$$

$$\text{Model 2:}\quad \log(C_{BAG}) = \text{intercept} + \beta_1 \log(C_w) \qquad (5)$$

where C_{BAG} was the personal exposures measured by the bag samples; C_w was the quantification result from the OP-FTIR measurements with bi-beam strategy; LOC was the subjects' locations either at Table A or Table B (where the latter table was assigned

TABLE I. Results from the Model 1 Building Process

	Model 1: Nose Height (R^2 = .93)			Model 1: Lapel Height (R^2 = .86)		
Predictors	**β[A]**	**SE[B]**	**p-value**	**β[A]**	**SE[B]**	**p-value**
Intercept	0.423	0.15	0.01	0.690	0.28	0.00
log(C_w)	0.894	0.69	0.00	0.762	0.43	0.00
LOC	0.001	−0.08	0.98	−0.170	−0.27	0.00
TASK	−0.023	−0.09	0.45	−0.038	−0.13	0.39
SUBJ	0.052[C]	0.05[D]	0.10[E]	0.096[C]	0.07[D]	0.06[E]

Note: The dependent variable is the log-transformed personal exposures measured by the bag samples.
[A]Coefficient estimated from the model building process.
[B]Standard error.
[C]Root-mean-square values of the coefficients for the five Subject dummy variables.
[D]Mean values of the standard errors for the five Subject dummy variables.
[E]p-values calculated from multiple partial F-test, representing the combined significance of the Subject variables.

as the baseline category); TASK was subjects' tasks for either the painting task or assembly task (where the latter task was assigned as the baseline category); SUBJ was a categorical variable for subjects. Because there were six subjects, a total of 5 (i=1∼5) dummy variables were included in the model. Model 1 was used to evaluate the importance of these covariates (i.e., subjects, locations, and tasks). Model 2 represented the worst scenario in which only OP-FTIR measurements were available and there was no information on the characteristics of other covariates. Analogous untransformed models also were fit, but the decision was made to use only the log-transformed models; the residual analysis showed that log transforming the measurements helped to improve the assumption of normality. This was confirmed by visually inspecting the residual plots, and by the Shapiro-Wilk statistics of the studentized residuals.[18]

By the end of the main exposure experiments, there was a total of 96 groups of samples (6 subjects × 8 rounds × 2 sessions). Each group of samples had 9 min of a lapel height bag sample, a nose height bag sample, and the corresponding OP-FTIR measurements. In GLM the dependent observations (the C_{BAG} variable) should be independent of one another.[18] However, in the present experiments one can argue that for each session the results from rounds 1, 2, 5, and 6 are similar to the results from rounds 3, 4, 7, and 8, respectively. Therefore, the average values from rounds 1 and 3, 2 and 4, 5 and 7, and 6 and 8 for C_{BAG} and C_w quantification results were used in the model. This reduced the number of data groups to 48.

The data were further split into two sets. For each subject the data collected during one of the sessions were randomly assigned to be the model-building set and the data collected during the other session to be the validation set. This data splitting approach was applied here for model validation purposes.[18] The model-building set was used first to build the model with the GLM procedure. This model was used to compute predicted values $\{C_{BAGi1}^*\}$ for this model-building set, i=1, 2, . . . , n_1; and also the predicted values $\{C_{BAGi2}^*\}$ for the validation set, i=n_1+1, n_1+2, . . . , n_1+n_2. Three parameters were used here to evaluate the performance of this model: **(1)** Bias is defined as the average of ($C_{BAG2} - C_{BAG2}^*$), where C_{BAG2} are the observed values in the validation set; **(2)** precision is defined as the standard deviation of ($C_{BAG2} - C_{BAG2}^*$); **(3)** shrinkage on cross-validation[18] is defined as $R^2(1) - R^2(2)$ where $R^2(1)$ = squared correlation coefficient of (logC_{BAG1}, logC_{BAG1}^*); C_{BAG1} were the observed values in the model-building set; $R^2(2)$ = squared correlation coefficient of (logC_{BAG2}, logC_{BAG2}^*). The quantity $R^2(2)$ is called the cross-validation correlation.

RESULTS AND DISCUSSION

Calibration Experiments

In the calibration experiments the average concentration for all 16 bag samples was 19.97 ppm ± 0.67 ppm. The small standard deviation suggests that N_2O was uniformly distributed inside the chamber. For Table A the mean ratio of OP-FTIR to bag samples was 1.02, very close to 1. However, at Table B the OP-FTIR somewhat underestimated the bag samples. The mean ratio of OP-FTIR to bag samples was 0.84. To make the results from the OP-FTIR and bag samples comparable at all locations, the obtained OP-FTIR concentrations in the main exposure experiments were divided by the mean ratios mentioned previously.

Model Building—Nose Height

In the main exposure experiments the mean N_2O concentration at the nose height of the model-building set was 27 ppm and 14 ppm for bag samples and OP-FTIR measurements, respectively. The OP-FTIR substantially underestimated the point samples, although one should keep in mind that this kind of univariate descriptive analysis does not consider the effects from other factors (e.g., differences of tasks and locations).

Table I summarizes the results from the Model 1 building process. Model 1 fits the data reasonably well with fitted R^2 values of 0.93. At nose height, C_w was the only significant predictor, and the other three covariates (LOC, TASK and SUBJ) were not significant predictors (Table I). This suggests that when the OP-FTIR with the bi-beam geometry is used to evaluate personal exposures at nose height, there is no need to collect information about the differences among different locations, tasks, and subjects. This makes this approach very attractive because information about the characteristics of these variables usually is not known. When only the C_w variable was included in Model 2, the R^2 value decreased slightly to 0.87. Figure 4 shows the correlation between the C_{BAG} samples and the OP-FTIR measurements. The first order regression line represents the predictions from Model 2. The obtained β_1 coefficient is 0.90 with the standard error of 0.08. The empirical regression line for Model 2 at the nose height given in Figure 4 is

$$\log(C_{BAG}) = 0.41 + 0.90 \times \log(C_w) \quad \textbf{(6)}$$

If we anti-log transform this empirical regression line, it can be rewritten as

$$C_{BAG} = 10^{0.41} \times 10^{0.90 \times \log(C_w)} = 2.6 \times C_w^{0.9} \quad \textbf{(7)}$$

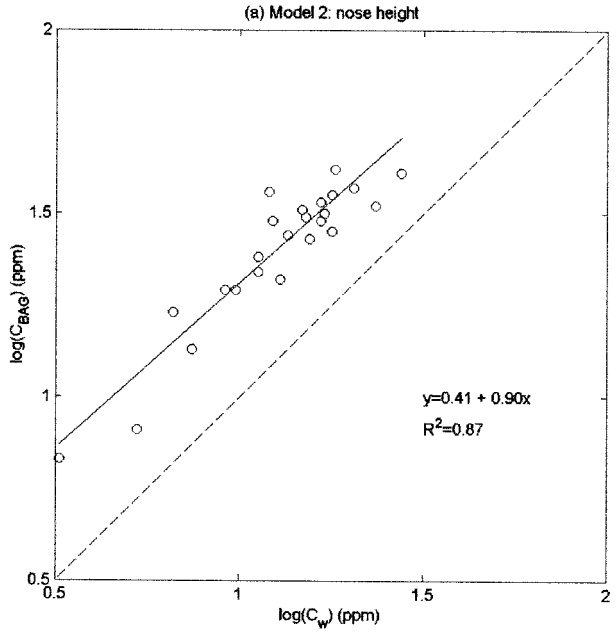

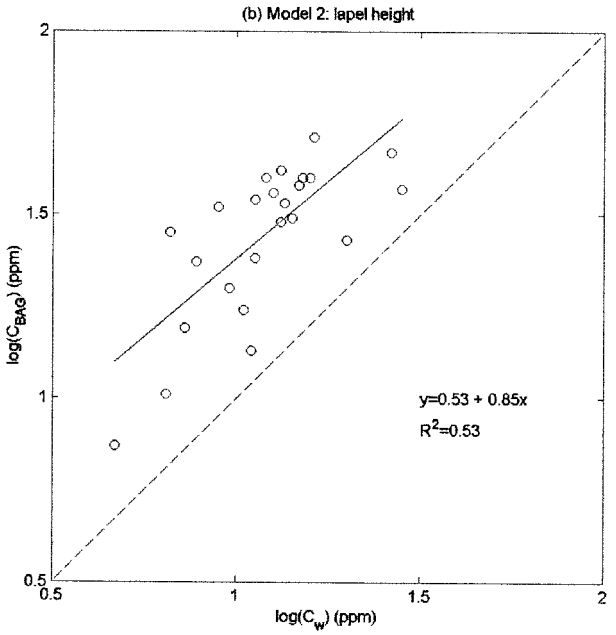

FIGURE 4. Results from the Model 2 building process. The x-axis represents the estimated personal exposures from the OP-FTIR measurements. The y-axis represents the measured personal exposures from the bag samples. (a) Linear regression model at nose height; (b) linear regression model at the lapel height.

Because the 95% CI of the slope 0.90 in Equation 6 is between 0.74 and 1.16, which contains 1, for the purpose of interpretation Equation 7 can be further simplified to:

$$C_{BAG} \approx 2.6 \times C_w \quad (8)$$

As Equation 8 indicates, the slope of the regression line (referred to as the "correction factor" in the following paragraph) between the OP-FTIR estimates and the point samples is not one. This is probably due to the fact that the C_{BAG} variable represents only one sampling point near the workers' nose, whereas the C_w represents a wider segmenting region in front of the workers' breathing zone. The magnitude of the correction factor depends on the mixing conditions at the sampling region. Yost et al.[15] suggested using a mixing factor, gamma (γ), to represent the mixing conditions along a beampath. Gamma is bounded between L_i/L_w and 1, where L_i is the path length of the assumed control segment (breathing zone) of fixed size, and L_w is the total beam path containing N control segments. Each control segment is assumed to contain a homogeneous concentration. A gamma of $L_i/L_w=1/N$ represents the condition of perfect mixing along the beam path, whereas a gamma of 1 represents the condition in which all the contaminant resides in only one segment. In the experimental set-up the beam path L_w was 90 cm. In industrial hygiene practice it usually is assumed that the personal samples represent the concentration levels at the breathing zone, which was previously defined as a 30-cm (1-ft) hemisphere from the nose.[15] Using 30 cm for the length L_i gives an estimate of N=3 (=90 cm/30 cm) control segments along the beam path L_w. This provides a lower and upper bound on the mixing factor gamma, which would have an estimated range between 0.33 (=30 cm/90 cm) and 1. The experimental results suggest that the correction factor in Equation 8 is correlated with $\gamma \times N$. Theoretically, in a condition of perfect mixing (γ=0.33) along the 90-cm beam path, Equation 8 should be $C_{BAG} = \gamma \times N \times C_w = C_w$. When all the contaminant resides in only one of the three control segments (γ=1), Equation 8 should be $C_{BAG} = \gamma \times N \times C_w = 3 \times C_w$. In the present study gamma was 2.6/3 = 0.87, suggesting a poorly mixed condition at the workstations. Combining the gamma model with the bi-beam measurements suggests an alternative way to place an upper and lower bound on the exposure at the workstation. Note that these bounding estimates of exposure can be made even if no bag samples are available.

Certainly, the estimated upper bound of the correction factor depends on the assigned size (L_i) of the breathing zone. A shorter L_i would increase the number (N) of control segments, thus having a higher estimation of the upper bound. For example, if the L_i equals 9 cm (instead of 30 cm) and the L_w is still 90 cm, the estimated correction factor would be bounded between 1 to 10. However, it is not reasonable to assume the L_i to be much smaller than the width of a person's head. In this kind of extreme condition (i.e., a very narrow plume or a tiny breathing zone), even a traditional point sampler located at the lapel would likely have difficulty capturing the exposure levels near the nose. One way to decrease the range of the estimated correction factor is by shortening L_w. If a very narrow plume is expected, using the same L_i (9 cm) in the above example and a shorter L_w of 45 cm (instead of 90 cm) would estimate the upper bound for the correction factor to be 5 (instead of 10).

Model Building—Lapel Height

The mean N_2O concentration at the lapel height of the model-building set was 30 ppm and 13 ppm for bag samples and OP-FTIR measurements, respectively. As in the results at the nose height, the OP-FTIR underestimated the point samples. The fitted R^2 value is 0.86 for Model 1 at the lapel height (Table I). In addition to the OP-FTIR measurements, LOC also was a significant predictor (Table I). This makes this model less attractive because more information about the characteristics of various locations must be collected to have useful exposure estimates. This explains why the R^2 value in Model 2 decreased dramatically to 0.53 (Figure 4b). It seems likely that placing the beams too

low introduced sampling errors due to transport and entrainment of contaminants in the body wake zone,[19] which does not reflect mixing conditions near the nose. However, the main interest for the industrial hygienist is the concentration levels directly in a workers' breathing zone. Because the concentrations at the nose height can be estimated accurately from the OP-FTIR measurements, this demonstrates the feasibility of using OP-FTIR for exposure assessments, although clearly the beams must be located near the plane of the breathing region to provide reliable data.

Model Validation

From the model-building process it was found that the OP-FTIR with a bi-beam sampling strategy was more practical and representative for estimating personal exposures at the nose height than at the lapel height. Therefore, the following validation analysis focused on the nose-height data only.

For the validation set, the cross-validation correlation $R^2(2)$ is 0.72. Subtracting this value from the squared correlation coefficient of 0.86 in model-building set, the estimated shrinkage on cross-validation of 0.14 for the log-transformed data is obtained. This shrinkage value indicates that this is a reasonably reliable model. The bias of this model for the validation data set is 0.7 ppm, and the precision is 5.5 ppm. Given that the mean value of the measured bag samples is 26.4 ppm, this is a relatively small bias (3%). The relatively low precision (20.7%) is partially due to small sample size (n=24).

In addition to treating each of the four possible task/worktable combinations separately for each subject when verifying the performance of this model, each subject's exposure levels can be estimated during the whole experimental period (1.75 hours). In other words, the experiments can be treated as scenarios when each worker has to perform two different tasks at two workstations, and the purpose is to estimate personal exposures from the bi-beam sampling strategy for the total sampling period. For these scenarios the range of the difference between the observed and predicted personal exposures among the six subjects is −2.5 to 5 ppm (standard deviation=2.8 ppm). This shows that the bi-beam sampling strategy also can be applied to estimate longer-term average exposures when workers have to move between different workstations.

In this study the 9-min average values of the C_w were used to represent the exposure levels estimated from the OP-FTIR measurements. Future studies could look at the distributions of the OP-FTIR measurements during the 9-min period and decide whether the mean, median, or other statistics are the most representative parameter. This may help to improve the correlation between the C_w and C_{BAG} or even bring the slope of the regression model closer to 1. The variance of these OP-FTIR measurements over time also should be considered while building the model. In addition, the bootstrap procedure as discussed in Tsai et al. could be incorporated.[20]

CONCLUSION

This study demonstrated that the bi-beam sampling strategy did not require additional information about the characteristics of locations, subjects, and tasks, and still produced a reliable and unbiased empirical exposure model. However, the fact that the correction factor between the C_w and C_{BAG} is not 1 somewhat limits this sampling technique. To apply this bi-beam technique in the field, two different approaches seem possible here:

(1) When the calibration experiments (i.e., comparing point samples and OP-FTIR measurements) are available for certain working conditions, the slope of the regression model can be obtained from the experimental data and then be used in the future for estimating personal exposures with the bi-beam sampling strategy. **(2)** When calibration experiments are not available, by applying the gamma model to place bounds on the mixing factor at the workstations, the slope of the regression model still can be estimated. To get a more precise estimation of the gamma, it is necessary to decrease the segmenting length (L_w in Figure 1) of the OP-FTIR in the breathing zone, because gamma is bounded between L_i/L_w and 1.

One required condition for applying the bi-beam sampling strategy is to have some restriction of the workers' locations, that is, they stay at fixed workstations during the sampling period. When the workers are completely mobile, further studies are needed and should consider incorporating the technique of computed tomography to measure concentrations over an area.

REFERENCES

1. **Hanst, P.L., and S.T. Hanst:** Gas measurement in the fundamental infrared region. In M.W. Sigrist, editor, *Air Monitoring by Spectroscopic Techniques.* New York: John Wiley & Sons, Inc., 1994.
2. **Herget, W.F., and J.D. Brasher:** Remote measurement of gaseous pollutant concentrations using a mobile Fourier transform interferometer system. *Appl. Opt. 18*:3404–3420 (1979).
3. **Levine, S.P., L.S. Ying, C.R. Strang, and H.K. Xiao:** Advantages and disadvantages in the use of Fourier transform infrared (FTIR) and filter infrared (FIT) spectrometers for monitoring airborne gases and vapors of industrial hygiene concern. *Appl. Ind. Hyg. 4*:180(1989).
4. **Yost, M.G., H.K. Xiao, R.C. Spear, and S.P. Levine:** Comparative testing of an FTIR remote optical sensor with area samplers in a controlled ventilation chamber. *Am. Ind. Hyg. Assoc. J. 53*:611–6 (1992).
5. **Farhat, S.K., and L.A. Todd:** Evaluation of open-path FTIR spectrometers for monitoring multiple chemicals in air. *Appl. Occup. Environ. Hyg. 15*:911–923 (2000).
6. **Todd, L., and D. Leith:** Remote-sensing and computed-tomography in industrial-hygiene. *Am. Ind. Hyg. Assoc. J. 51*:224–233 (1990).
7. **Todd, L., and G. Ramachandran:** Evaluation of optical source-detector configurations for tomographic reconstruction of chemical concentrations in indoor air. *Am. Ind. Hyg. Assoc. J. 55*:1133–43 (1994).
8. **Samanta, A., and L.A. Todd:** Mapping air contaminants indoors using a prototype computed tomography system. *Ann. Occup. Hyg. 40*: 675–91 (1996).
9. **Bhattacharyya, R., and L.A. Todd:** Spatial and temporal visualization of gases and vapours in air using computed tomography. Numerical studies. *Ann. Occup. Hyg. 41*(1):105–22 (1997).
10. **Park, D.Y., M.G. Yost, and S.P. Levine:** Evaluation of virtual source beam configurations for rapid tomographic reconstruction of gas and vapor concentrations in workplaces. *J. Air Waste Manage. Assoc. 47*: 582–591 (1997).
11. **Price, P.N.:** Pollutant tomography using integrated concentration data from non-intersecting optical paths. *Atmos. Environ. 33*:275–280 (1999).
12. **Hashmonay, R.A., M.G. Yost, and C.F. Wu:** Computed tomography of air pollutants using radial scanning path-integrated optical remote sensing. *Atmos. Environ. 33*:267–274 (1999).
13. **Wu, C.F., M.G. Yost, R.A. Hashmonay, and D.Y. Park:** Experimental evaluation of a radial beam geometry for mapping air pollutants using optical remote sensing and computed tomography. *Atmos. Environ. 33*:4709–4716 (1999).
14. **Todd, L.A.:** Mapping the air in real-time to visualize the flow of gases and vapors: Occupational and environmental applications. *Appl. Occup. Environ. Hyg. 15*:106–13 (2000).
15. **Yost, M.G., R.A. Hashmonay, Y. Zhou, R. Spear, D.Y. Park, and**

S.P. Levine: Estimating maximum concentrations for open path monitoring along a fixed beam path. *J. Air Waste Manage. Assoc. 49*:424–433 (1999).

16. **Ross, K.R. and L.A. Todd:** Field evaluation of a transportable open-path FTIR spectrometer for real-time air monitoring. *Appl. Occup. Environ. Hyg. 17*:131–143 (2002).
17. **Haaland, D.M., and R.G. Easterling:** Application of new least-squares methods for the quantitative infrared analysis of multicomponent samples. *Appl. Spectrosc. 36*:665–672 (1982).
18. **Kleinbaum, D.G., L.L. Kupper, and K.E. Muller:** *Applied Regression Analysis and Other Multivariable Methods,* 2nd ed. Boston, Mass.: PWS-Kent Publishing, 1988.
19. **Kim, T., and M.R. Flynn:** Airflow pattern around a worker in a uniform freestream. *Am. Ind. Hyg. Assoc. J. 52*:287–296 (1991).
20. **Tsai, M.Y., M.G. Yost, C.F. Wu, R.A. Hashmonay, and T.V. Larson:** Line profile reconstruction: Validation and comparison of reconstruction methods. *Atmos. Environ. 35*:4791–4799 (2001).